Milestoning estimators of dissipation in systems observed at a coarse resolution: When ignorance is truly bliss

Kristian Blom,[1] Kevin Song,[2] Etienne Vouga,[2] Aljaž Godec,[1, *] and Dmitrii E. Makarov[3, †]

[1]*Mathematical bioPhysics group, Max Planck Institute for Multidisciplinary Sciences, Göttingen 37077, Germany*
[2]*Department of Computer Science, University of Texas at Austin, Austin, Texas 78712, USA*
[3]*Department of Chemistry and Oden Institute for Computational Engineering and Sciences,*
The University of Texas at Austin, Austin, Texas 78712, USA
(Dated: October 12, 2023)

Many non-equilibrium, active processes are observed at a coarse-grained level, where different microscopic configurations are projected onto the same observable state. Such "lumped" observables display memory, and in many cases the irreversible character of the underlying microscopic dynamics becomes blurred, e.g., when the projection hides dissipative cycles. As a result, the observations appear less irreversible, and it is very challenging to infer the degree of broken time-reversal symmetry. Here we show, contrary to intuition, that by ignoring parts of the already coarse-grained state space we may —via a process called milestoning— improve entropy-production estimates. Milestoning systematically renders observations "closer to underlying microscopic dynamics" and thereby improves thermodynamic inference from lumped data assuming a given range of memory. Moreover, whereas the correct general physical definition of time-reversal in the presence of memory remains unknown, we here show by means of systematic, physically relevant examples that at least for semi-Markov processes of first and second order, waiting-time contributions arising from adopting a naive Markovian definition of time-reversal generally must be discarded.

One-sentence summary: Non-equilibrium processes are often observed at a coarse resolution, blurring the irreversibility of dynamics; contrary to intuition, we show that systematically increasing ignorance via a process called milestoning can improve thermodynamic inference.

INTRODUCTION

Although the nonequilibrium character of active systems may often be self-evident (e.g., the directed motion of a kinesin motor or persistent rotation of the F_1-ATPase [1]), differentiating in general between equilibrium and non-equilibrium steady states at mesoscopic and microscopic scales is surprisingly difficult [2–6]. A key reason is that a broken time-reversal symmetry often emerges on length scales where detailed microscopic information is unavailable, e.g., below the diffraction limit. In particular, single-molecule experiments probe inherently coarse-grained representations of microscopic dynamics [7] and may thus underestimate [2] or even "be blind to" relevant slow dissipative degrees of freedom [8].

Coarse-graining may be a consequence of experimental limitations as well as of data analysis: for example, the location of a microscopic probe is, most optimistically, limited by the pixel size, which introduces spatial coarse-graining [9]. Similarly, when protein folding is probed using optical tweezers [10] or fluorescence resonance energy transfer [2, 11, 12], many molecular conformations with, respectively, the same extension or with the same
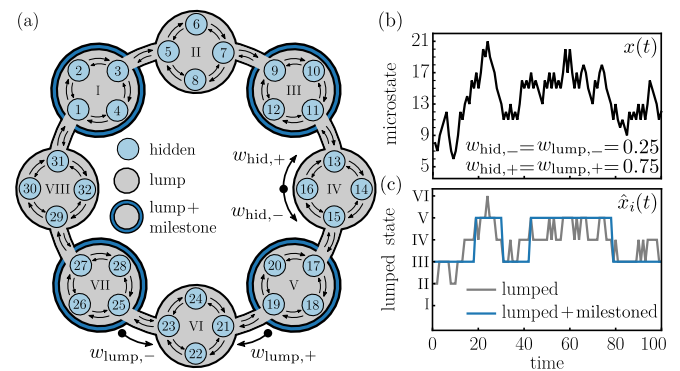
FIG. 1. **Lumping and milestoning a discrete-state Markov chain.** (a) Schematic of a discrete-state Markov chain with 32 hidden microstates lumped into domains I-VIII (gray) each containing 4 microstates. Such a partitioning arises naturally when the underlying process is observed with coarse resolution. Milestoning involves further post-processing of the lumped process: some lumped states (here, the domains I, III, V, and VII) are declared to be milestones (blue). Once the trajectory enters a milestone, the coarse-grained state of the milestone trajectory remains in said milestone until it enters a different milestone. (b) Trajectory of the full Markov chain $x(t)$. (c) Trajectory of the coarse-grained semi-Markov chain $\hat{x}_i(t)$ obtained by lumping (gray) and further milestoning (blue).

distance between fluorescent probes are lumped onto a single state. This projects the high-dimensional conformational dynamics onto a single lumped coordinate.

Consider the total steady-state entropy-production rate (i.e., dissipation rate), estimated as [13, 14]

$$\langle \dot{S}[x] \rangle \equiv \lim_{t \to \infty} \frac{1}{t} \left\langle \ln \left(\frac{P[\{x(\tau)\}_{0 \le \tau \le t}]}{P[\{\theta x(\tau)\}_{0 \le \tau \le t}]} \right) \right\rangle, \quad (1)$$

where $x(\tau)$ denotes the system's state at time τ, $P[\{x(\tau)\}_{0\leq\tau\leq t}]$ is the probability of a forward path $\{x(\tau)\}_{0\leq\tau\leq t}$ and θ denotes the *physically consistent* time-reversal operation, such that $P[\{\theta x(\tau)\}_{0\leq\tau\leq t}]$ corresponds to the probability of the time-reversed path. In Eq. (1) Boltzmann's constant was set to 1, $\langle\cdot\rangle$ indicates averaging over $P[\{x(\tau)\}_{0\leq\tau\leq t}]$, and we tacitly assumed that the dynamics is ergodic. When $x(\tau)$ is a Markov process, $\{\theta x(\tau)\}_{0\leq\tau\leq t} = \{\epsilon x(t-\tau)\}_{0\leq\tau\leq t}$ where ϵ denotes that we must simultaneously change the sign of all degrees of freedom that are *odd* under time reversal (such as momenta).

Note that in the presence of memory, the physically consistent form of time-reversal θ is generally *not* known. In particular, even in the absence of momenta one *cannot* simply assume the Markov definition, i.e., $\{\theta x(\tau)\}_{0\leq\tau\leq t} \neq \{x(t-\tau)\}_{0\leq\tau\leq t}$ (see [15–17] and counterexamples below). Memory effects require adapted definitions of time reversal, analogous to momenta in inertial systems [16, 17]. In particular, naively setting $\{\theta x(\tau)\}_{0\leq\tau\leq t}\overset{!}{=}\{x(t-\tau)\}_{0\leq\tau\leq t}$ in Eq. (1) may yield a positive entropy production for coarse-grained representations of manifestly reversible microscopic dynamics, as it leads to a "waiting-time contribution" to dissipation [15–17].

If the time-reversal operation and coarse-graining are carried out correctly, projected representations of microscopic dynamics are usually "less irreversible" than the true dynamics [16, 18–22]. That is, if a coarse-grained representation $\hat{x}(t)$ of the full dynamics is considered, we typically expect to underestimate [23] the true entropy production [16, 18, 19, 24], i.e.

$$0 \leq \langle\dot{S}[\hat{x}]\rangle \leq \langle\dot{S}[x]\rangle. \qquad (2)$$

Recently, there has been a surge in interest in thermodynamic inference from coarse-grained, partially observed dynamics [16, 19, 20, 22, 25–27]. The arguably most direct method to infer a lower bound on the entropy production is via the thermodynamic uncertainty relation (TUR) [9, 28–40]. Moreover, approaches were developed that exploit the information encoded in the non-Markovian character to infer bounds on dissipation [21, 22, 41–43].

Given the inequality in Eq. (2), optimal estimation of entropy production from experimental observations remains an open question. Indeed, different coarse-grained representations yield different estimates; moreover, in any realistic experimental setting neither the microscopic dynamics nor the precise coarse-graining is known. Recently, it was found that a coarse-graining method called "milestoning" preserves the microscopic entropy production even in the absence of a time-scale separation between hidden and observed degrees of freedom, if no dissipative cycles are hidden [16, 44]. In contrast, the more common coarse-graining approach called "lumping" (see Fig. 1 and [18]) in general may underestimate $\langle\dot{S}[x]\rangle$ even in the presence of such time-scale separation [44]. Milestoning, originally developed as a method for efficient

computation [45–47], projects the dynamics onto "hopping" between a set of milestones that do not cover the entire configuration space, thereby mapping continuous or discrete-state "microscopic" dynamics onto a generally non-Markovian random walk. Intriguingly, we here show that milestoning, if used to post-process lumped dynamics, can improve thermodynamic inference. In other words, milestone trajectories, obtained by *discarding* certain details of lumped trajectories (as in Fig. 1), can provide improved estimates of dissipation; as such, milestoning analysis is directly applicable to experimentally observed dynamics, which are inherently lumped.

Here we focus on the direct approach (1) and demonstrate that, contrary to naive intuition, milestoning already lumped dynamics may improve entropy-production estimates via Eq. (1) *given the same coarse-grained trajectories and even in the presence of hidden cycles*. That is, by ignoring parts of the coarse-grained state space and thus introducing additional "controlled ignorance" we actually render the trajectory "closer to the underlying microscopic dynamics" and thereby improve the dissipation estimator (1) [48]. We explicitly address the scenario where lumping hides dissipative cycles and compare the milestoning estimate with the bound inferred from the TUR. We show how post-lumped milestoning may be used systematically to improve thermodynamic inference, i.e., to enhance the precision of estimating dissipation from coarse observations. We stress the importance of considering a physically consistent time-reversal operation in the presence of memory, and show that asymmetric waiting-time contributions that emerge upon milestoning generally do not contribute to dissipation.

MILESTONING DYNAMICS WITH HIDDEN CYCLES

We begin with a toy model that contains hidden dissipative cycles (see [49–51] for similar toy models). Models of this kind can emerge as descriptions of a system of magnetically coupled colloidal particles [8, 52], chemical reaction networks [53], circular hidden Markov models [54, 55], and molecular conformation dynamics [3]. Here we consider a discrete-time Markov process as shown in Fig. 1a. The observed dynamics involves N_{lump} observable states arranged along a ring, and each such observable state contains N_{hid} microscopic states forming a ring (see Fig. 1a). Within each lump there are two maximally separated microstates which are connected to the previous/next lump (e.g., microstate 3 and 5 in Fig. 1a), and in the SM we also consider the case with three microstates connected between the lumps. The transition probabilities for internal microstates (i.e., microstates not connecting two lumps) are $w_{\mathrm{hid},+}$ in the clockwise direction, and $w_{\mathrm{hid},-}$ in the counterclockwise direction. For microstates connecting two lumps, we have $w_{\mathrm{lump},\pm}$ for transitions between the lumps, and $(1-w_{\mathrm{lump},\pm})w_{\mathrm{hid},\pm}$ for internal transitions. Thus, for $w_{\mathrm{hid},+} \neq w_{\mathrm{hid},-}$, lump-
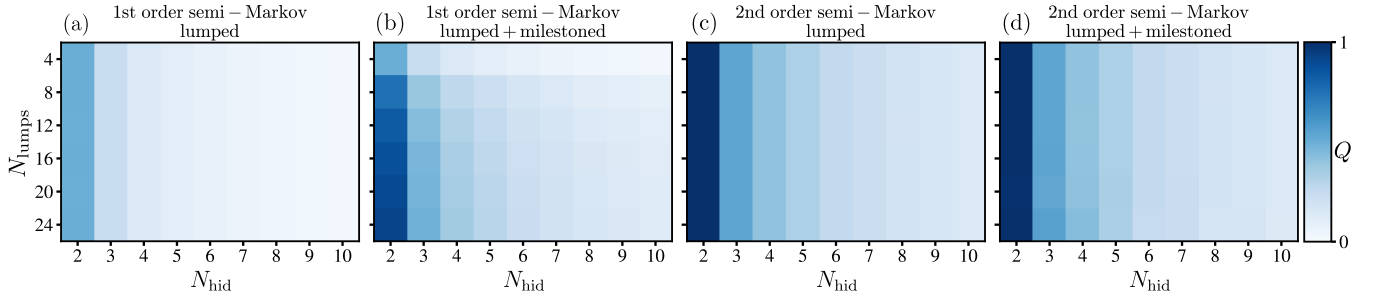
FIG. 2. **Estimating the entropy production from a coarse-grained trajectory with hidden cycles.** The diffusive trajectory is governed by the discrete-state ring-like Markov chain shown in Fig. 1, with N_{lumps} the number of lumped states, N_{hid} the number of hidden microstates per lumped state, transition rates $\{w_{\text{hid},+}, w_{\text{hid},-}\} = \{w_{\text{lump},+}, w_{\text{lump},-}\} = \{0.6, 0.4\}$, and 10^8 discrete steps. (a, c) Quality factor Q given by Eq. (5) for the entropy production estimated with the lumped trajectory assuming 1$^{\text{st}}$ order semi-Markov (see Eq. (3)) (a) and 2$^{\text{nd}}$ order semi-Markov (see Eq. (4)) (c). (b, d) Quality factor for the entropy production estimated with the post-lumped milestoned trajectory with 4 equidistant milestones, assuming 1$^{\text{st}}$ order semi-Markov (b) and 2$^{\text{nd}}$ order semi-Markov (d).

ing the N_{hid} states into a single observable state hides dissipative cycles when $N_{\text{hid}} > 2$. A microscopic and lumped trajectory are shown in Fig. 1b and c (gray line), respectively. We now milestone the trajectory by taking 4 equidistant lumps as milestones (see Fig. 1a and Fig. 1c blue line).

To evaluate $\langle \dot{S}[\hat{x}_i] \rangle$, where the subscript $i = \{\text{lump}, \text{mil}\}$ indicates whether the entropy production is estimated for the lumped trajectory or the milestone trajectory, we use Eq. (1) and measure lump/milestone-sequence frequencies in the trajectory [56, 57]. In the presence of long-range memory this is a computationally demanding task requiring many independent steady-state trajectories or one extremely long trajectory. Even if this is given, a finite range of memory must be assumed in practical computations of path probabilities $P[\{x(\tau)\}_{0 \leq \tau \leq t}]$ and $P[\{\theta x(\tau)\}_{0 \leq \tau \leq t}]$. A numerical implementation of the inference is provided in [58].

Note that $\hat{x}_i(t)$ in Fig. 1c is indeed a non-Markovian process. This is manifested in the fact that the estimate of $\langle \dot{S}[\hat{x}_i] \rangle$ strongly depends on the assumption of the underlying extent of memory. That is, considering only the preceding step—in the 1$^{\text{st}}$ order semi-Markov approximation—we assume that $\hat{x}_i(t)$ depends only on $\hat{x}_i(t-1)$ but not on $\hat{x}_i(t-k)$ for $k \geq 2$, leading to the one-step affinity estimate (assuming all coarse states and milestones are equivalent as in Fig. 1a)

$$\langle \dot{S}_1^{\text{aff}}[\hat{x}_i] \rangle = \frac{p_+^i - p_-^i}{\langle \tau_i \rangle} \ln\left(\frac{p_+^i}{p_-^i}\right), \tag{3}$$

where $\langle \tau_i \rangle$ is the average waiting time within a coarse-grained state, and $p_\pm^i$ are the forward/clockwise $(+)$ and backward/counterclockwise $(-)$ jump probabilities in the sequence of *distinct* coarse-grained states (i.e., upon removing repeated consecutive coarse-grained states).

In the kth order semi-Markov approximation we assume that the probability of $\hat{x}_i(t)$ depends on the sequence $\{\hat{x}_i(t-1), \ldots, \hat{x}_i(t-k)\}$. To be concrete, $\hat{x}_i(t)$ in Fig. 1c is a 2$^{\text{nd}}$ order semi-Markov process [41] (see

also [42, 43]), where the jump probabilities *and* waiting times depend on the previous state. Naively, taking $\{\theta \hat{x}(\tau)\}_{0 \leq \tau \leq t} \overset{!}{=} \{\hat{x}(t-\tau)\}_{0 \leq \tau \leq t}$ in Eq. (1), yields two contributions: the two-step affinity contribution $\langle \dot{S}_2^{\text{aff}}[\hat{x}_i] \rangle$, and a contribution of waiting times $\langle \dot{S}_2^{\text{wt}}[\hat{x}_i] \rangle$ [41]. In particular, for $\hat{x}_i(t)$ in Fig. 1c the two-step affinity contribution reads [41, 44]

$$\langle \dot{S}_2^{\text{aff}}[\hat{x}_i] \rangle = \frac{p_+^i - p_-^i}{\langle \tau_i \rangle} \ln\left(\frac{\phi_{++}^i}{\phi_{--}^i}\right), \tag{4}$$

where $\phi_{\pm\pm}^i$ are conditional splitting probabilities of making a forward/backward jump, given that the previous jump occurred in the forward/backward direction. The explicit form of the waiting-time contribution $\langle \dot{S}_2^{\text{wt}}[\hat{x}_i] \rangle$ (see Eq. (S1) below) suggests that as soon as waiting time distributions to make a forward versus a backward jump (conditioned on that the preceding jump has also occurred in the forward or backward direction, respectively) are not equal, these contribute to dissipation [41]. Below, however, we give examples where $\langle \dot{S}_2^{\text{wt}}[\hat{x}_i] \rangle > 0$ for systems obeying detailed balance; therefore, the naive Markovian time-reversal operation leading to $\langle \dot{S}_2^{\text{wt}}[\hat{x}_i] \rangle$ cannot be generally correct and does not necessarily measure dissipation. In anticipation that waiting times do *not* contribute to dissipation, we ignore them in the inference of $\langle \dot{S}_k[\hat{x}_i] \rangle$. Later, we also prove that they indeed result in a spurious contribution to the estimate for $\langle \dot{S}[x] \rangle$.

Taking a single *ergodically long* trajectory, we use Eq. (3) or Eq. (4) for the microscopic, lumped, and post-lump milestoned trajectories to estimate the entropy production. To determine the accuracy of the estimates, we calculate the quality factor $0 \leq Q \leq 1$, equal to the ratio of the estimated entropy production to the true entropy production of the microscopic process:

$$Q = \langle \dot{S}_k^{\text{aff}}[\hat{x}_i] \rangle / \langle \dot{S}[x] \rangle, \tag{5}$$

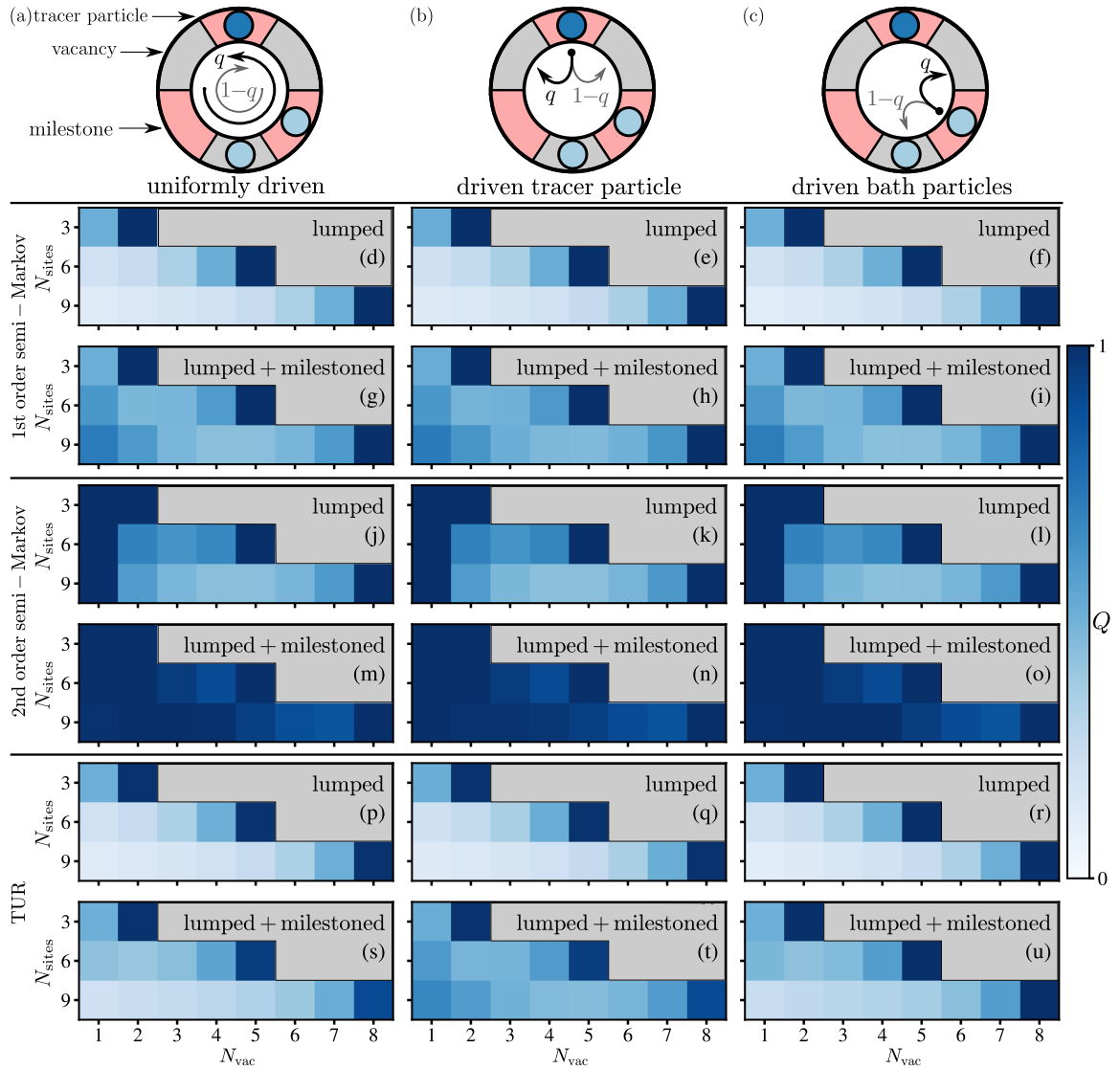where $i = \{\text{lump}, \text{mil}\}$. We apply the 1$^{\text{st}}$ order (i.e.,

FIG. 3. **Estimating the entropy production in single-file diffusion for different driving schemes.** (a-c) Schematic of the different driving scenarios, where the tracer particle is indicated in dark blue, and bath particles in light blue. Red sites indicate the milestone positions for the tracer particle. Asymmetric transition rates are $\{1-q, q\}=\{0.55, 0.45\}$. In the schematics $N_{\text{sites}}=6$ and $N_{\text{vac}}=3$. (d-i) Quality factor of the entropy production estimated with the 1st order semi-Markov approximation (see Eq. (3)). (j-o) Quality factor of the entropy production estimated with the 2nd order semi-Markov approximation (see Eq. (4)). (p-u) Quality factor of the entropy production estimated with the discrete-time TUR given by Eq. (6) using the tracer particle current.

$k = 1$) semi-Markov and 2nd order (i.e., $k = 2$) semi-Markov approximation to estimate $\langle \dot{S}[\hat{x}_i] \rangle$, and the results are shown in Fig. 2. For $N_{\text{hid}} \geq 3$ the estimates from both coarse-grained trajectories (i.e., lumped and milestoned) are significantly lower than the true entropy-production rate. This is due to the presence of hidden dissipative cycles. Nevertheless, within the 1st order semi-Markov approximation milestoning the lumped trajectory improves the entropy-production estimate (compare Figs. 2a,b). On the 2nd order semi-Markov level milestoning does not improve the estimate (Figs. 2c,d), since the sequence of lumps (milestones, respectively) is

exactly a 2nd order semi-Markov chain.

When there are no hidden cycles, i.e., for $N_{\text{hid}} = 2$, we recover the exact microscopic entropy production with Eq. (4) which, notably, does *not* take into account the waiting-time contribution, i.e. $\langle \dot{S}_2^{\text{aff}}[\hat{x}_i] \rangle = \langle \dot{S}[x] \rangle$. In fact, since $\langle \dot{S}_2^{\text{wt}}[\hat{x}_{\text{mil}}] \rangle \geq 0$ for asymmetrically placed milestones, including the waiting-time contribution from [41] violates the condition (2) and may erroneously yield a positive entropy production even when the microscopic dynamics obeys detailed balance (see SM). This underscores that Eq. (1) with $\{\theta \hat{x}(\tau)\}_{0 \leq \tau \leq t} \overset{!}{=} \{\hat{x}(t-\tau)\}_{0 \leq \tau \leq t}$ *a priori* does *not* measure violation of detailed balance

of processes with memory.

Interestingly, milestoning lumped dynamics may improve the entropy-production estimate even in the presence of hidden cycles if the range of memory is not captured exactly in the evaluation of Eq. (1). Notably, in practice the extent of memory is unlikely to be known, and computations at orders higher than 2 quickly become unfeasible.

DRIVEN SINGLE-FILE DIFFUSION

Next, we consider tracer-particle dynamics in discrete-time single-file diffusion on a ring (see Fig. 3), a paradigmatic model of dynamics with long memory and anomalous diffusion [59–65] as well as a paradigm for diffusion in crowded media [66–70] and transport through biological channels [71]. Let N_{sites} be the total number of sites on the ring, and N_{vac} the number of empty sites (vacancies), such that the total number of particles is $N = N_{\text{sites}} - N_{\text{vac}}$. At each discrete time step a particle is picked at random and shifted with a given probability to the left or right if the new site is unoccupied. Note that the latter condition introduces waiting times between jumps, i.e., it effectively gives rise to local Poissonian clocks in the limit of continuous time. We track the position of a tracer particle (see e.g., Fig. 3a, dark blue), which results in a lumped process, where multiple microscopic states correspond to the same location of the tracer particle but different arrangements of the unobserved "bath" particles.

We consider three different driving scenarios: (i) a uniformly driven system with clockwise (w_+) and counterclockwise (w_-) transition rates $\{w_+, w_-\}=\{1-q, q\}$ (Fig. 3a), (ii) a driven tracer particle with transition rates $\{w_+^{\text{t}}, w_-^{\text{t}}\}=\{1-q, q\}$ and bath particles with symmetric hopping rates $\{w_+, w_-\}=\{1/2, 1/2\}$ (Fig. 3b) [72–76], and (iii) the opposite scenario where the bath particles are driven, and the tracer particle hops symmetrically (Fig. 3c) [77].

We further consider 3 maximally separated post-lumped milestones on the ring (see e.g., Fig. 3a, red sites). This type of milestoning corresponds to that implemented in [44] and yields the exact entropy production in the case of a single particle [16, 44].

In each driving scenario we evaluate, numerically, the exact (microscopic) entropy production $\langle \dot{S}[x] \rangle$ and compare it with $\langle \dot{S}_k^{\text{aff}}[\hat{x}_i] \rangle$ assuming 1st order (i.e., $k = 1$) (Fig. 3d-i) and 2nd order (i.e., $k = 2$) semi-Markov (Fig. 3j-o) statistics for the lumped and post-lumped milestoned trajectories, respectively. For all driving scenarios, and both semi-Markov approximations, we find that milestoning of the lumped trajectories significantly improves the entropy-production estimate.

For a further comparison, we also estimate $\langle \dot{S}[\hat{x}_i] \rangle$ via the *discrete-time* TUR [78], which provides a universal trade-off between precision of any thermodynamic flux and dissipation in the system [28, 39, 78]. By determining the average $\langle J_i \rangle$ and variance $\text{var}(J_i)$ of the tracer-particle current in the lumped and post-lumped milestoned trajectories (see SM for details), the quality factor of the discrete-time TUR [78] estimate reads [78]

$$Q_{\text{TUR}} = \ln\left(2\langle J_i \rangle^2/\text{var}(J_i) + 1\right)/\langle \dot{S}[x] \rangle, \qquad (6)$$

and is shown in Fig. 3p-u. Note that for lumped dynamics it was proven that $0 \leq Q_{\text{TUR}} \leq 1$ [78], but is a priori not clear if the TUR holds also for the post-lumped milestoned dynamics. Here we simply assume this to be true, and find that the milestoned estimates outperform the lumped estimates (see bottom panel in Fig. 3).

INCREASING IGNORANCE

In Fig. 2b we observe that by increasing N_{lumps} at fixed N_{hid}, which increases the average distance between the milestones and hence our "ignorance", the 1st order estimate $\langle \dot{S}_1^{\text{aff}}[\hat{x}_{\text{mil}}] \rangle$ gradually improves. Similarly, in Fig. 3g-i we find that for larger N_{sites} (except for $N_{\text{sites}} - N_{\text{vac}} = 1$) the quality factor of the 1st order semi-Markov approximation is improved for the milestoned trajectory. On the contrary, the entropy estimates for the lumped dynamics deteriorate with increasing N_{sites} (see Fig. 3d-f). We now show, at first sight paradoxically, that when milestoning is used, a larger distance between milestones and hence "more ignorance" may indeed improve thermodynamic inference.

Let us focus on uniformly driven single-file diffusion with one vacancy, i.e. $N_{\text{vac}} = 1$, as shown in Fig. 4. For a given number of sites N_{sites}, there are $N_{\text{sites}} - 1$ microstates with a fixed location of the tracer particle. There are in total $N_{\text{sites}}(N_{\text{sites}} - 1)$ microscopic states, with groups of $N_{\text{sites}} - 1$ states forming the lumped states of the macroscopic system (i.e., the position of the
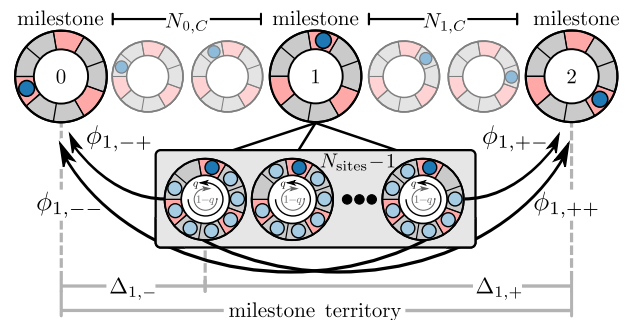

FIG. 4. **Splitting probabilities in milestoned single-file diffusion.** The upper panel depicts the lumped states, where we only observe the location of the tracer particle. The lower panel depicts the $N_{\text{sites}} - 1$ hidden microstates. Adjacent milestones are separated by $N_{j,C}(N_{\text{sites}} - 1)$ microscopic states. Here we have $N_{0,C} = N_{1,C} = 2$ and $N_{\text{sites}} = 9$. The random walk on milestones is an 2nd order semi-Markov process, with the sequence of milestones visited by the random walker determined by the splitting probabilities $\phi_{j,\pm\pm}$.

tracer particle). We now designate some of those coarse states to be milestones. Specifically, suppose we take 3 milestones with $N_{j,C}$ coarse states between milestone j (mod 3) and milestone $j+1$ (mod 3) (see Fig. 4). From here on we always take the index j modulo 3. Note that $N_{j,C}$ and N_{sites} are related by $\sum_j [1 + N_{j,C}] = N_{\text{sites}}$.

In the microscopic description of the problem, one can enumerate the microstates such that each milestone itself is composed of $N_{\text{sites}}-1$ states aligned along a line. We apply milestoning to obtain the trajectory $\hat{x}_{\text{mil}}(t)$ as described before: the position of the tracer particle corresponds to the last visited milestone, resulting in a 2nd order semi-Markov process. Specifically, the milestone sequence can be described by the conditional splitting probabilities *in the sequence of distinct states* (i.e. upon removing repeated consecutive milestoned states) $\{\phi_{j,++}, \phi_{j,+-}, \phi_{j,-+}, \phi_{j,--}\}$, where $\phi_{j,++}$, for example, is the conditional probability of making a step from milestone j to milestone $j+1$, given that the previous step occurred from milestone $j-1$ to milestone j.

To calculate the splitting probabilities $\phi_{j,++}$ and $\phi_{j,-+}$, for example, we consider the random walker starting in the leftmost state of the segment of $N_{\text{sites}}-1$ forming a milestone (see gray box in Fig. 4). If we denote this state by k, then $\phi_{j,-+}$ and $\phi_{j,++}$ are the probabilities to exit the interval $\{k - \Delta_{j,-}, ..., k + \Delta_{j,+}\}$ through its left and right boundaries with $\{\Delta_{j,-}, \Delta_{j,+}\} = \{N_{j-1,C}(N_{\text{sites}}-1)+1, (N_{j,C}+1)(N_{\text{sites}}-1)\}$. One may recognize that the solution to this problem is equivalent to solving the Gambler's ruin problem [79]. Specifically, if we let $\alpha_q \equiv q/(1-q)$, we obtain

$$\phi_{j,++} = (1-\alpha_q^{\Delta_{j,-}})/(1-\alpha_q^{\Delta_j}), \ \phi_{j,-+} = 1-\phi_{j,++},$$
$$\phi_{j,+-} = (1-\alpha_q^{\Delta_{j-1,+}})/(1-\alpha_q^{\Delta_j}), \ \phi_{j,--} = 1-\phi_{j,+-}. \quad (7)$$

where $\Delta_j = \Delta_{j,-} + \Delta_{j,+}$ denotes the territory of milestone j, i.e., the domain size the trajectory needs to exit upon entering another milestone. Given these splitting probabilities, we can determine the entropy production at the level of the 1st order semi-Markov approximation, which reads

$$\langle \dot{S}_1^{\text{aff}} \rangle = \frac{1}{\langle \tau \rangle} \sum_j [\pi_j p_{j,+} - \pi_{j+1} p_{j+1,-}] \ln\left(\frac{\pi_j p_{j,+}}{\pi_{j+1} p_{j+1,-}}\right), \quad (8)$$

where π_j is the steady-state probability in milestone j, $p_{j,\pm}$ the transition probability to jump from milestone j to $j \pm 1$, and $\langle \tau \rangle = \sum_j \langle \tau_j \rangle$ the total average waiting time in the milestones. Note that for equidistant milestones $\pi_j = 1/3$, and Eq. (S1) reduces to Eq. (3).

The steady-state and transition probabilities can be determined from the conditions

$$\pi_j = \pi_{j+1} p_{j+1,-} + \pi_{j-1} p_{j-1,+},$$
$$\pi_j p_{j,+} = \pi_{j-1} p_{j-1,+} \phi_{j,++} + \pi_{j+1} p_{j+1,-} \phi_{j,+-}, \quad (9)$$

together with $\sum_j \pi_j = 1$ and $p_{j,+} + p_{j,-} = 1$. Upon in-

serting Eq. (7) into Eq. (9) we find

$$\pi_j = (1 - \alpha_q^{\Delta_{j-1,-}})(1 - \alpha_q^{\Delta_{j,-}+\Delta_{j+1,-}})/\mathcal{N},$$
$$p_{j,+} = (1 - \alpha_q^{\Delta_{j,-}})/(1 - \alpha_q^{\Delta_{j,-}+\Delta_{j+1,-}}), \quad (10)$$

where $\mathcal{N} = \sum_j (1 - \alpha_q^{\Delta_{j-1,-}})(1 - \alpha_q^{\Delta_{j,-}+\Delta_{j+1,-}})$.

The average waiting time in a milestone can be split in two parts, with respect to entering the milestone from the left or the right. This yields

$$\langle \tau_j \rangle = \pi_{j-1} p_{j-1,+} \langle \tau_j^- \rangle + \pi_{j+1} p_{j+1,-} \langle \tau_j^+ \rangle, \quad (11)$$

where the average waiting times conditioned on starting from the left/right entrance of the milestone are given by (see page 4 in [79])

$$\langle \tau_j^- \rangle = (\Delta_{j,-} - \Delta_j \phi_{j,++}) N/(2q - 1),$$
$$\langle \tau_j^+ \rangle = (\Delta_{j-1,+} - \Delta_j \phi_{j,+-}) N/(2q - 1), \quad (12)$$

and lead to the total average waiting time in the milestones

$$\langle \tau \rangle = \frac{N \sum_j \Delta_{j,+}}{(1 - 2q)(3 - 2\sum_j 1/(1 - \alpha_q^{-\Delta_{j,-}}))}. \quad (13)$$

Inserting Eqs. (10) and (13) into Eq. (S1) we finally obtain the affinity contribution of the milestoned process within the 1st order semi-Markov approximation

$$\langle \dot{S}_1^{\text{aff}}[\hat{x}_{\text{mil}}] \rangle = \frac{3/(N_{\text{sites}} - 1) + \sum_j N_{j,C}}{3 + \sum_j N_{j,C}} \langle \dot{S}[x] \rangle$$
$$= \frac{3/(N_{\text{sites}} - 1) + N_{\text{sites}} - 3}{N_{\text{sites}}} \langle \dot{S}[x] \rangle \quad (14)$$

where $\langle \dot{S}[x] \rangle$ is the exact entropy production which can be obtained from the dynamics of the vacancy, and reads

$$\langle \dot{S}[x] \rangle = \frac{2q - 1}{N} \ln\left(\frac{q}{1 - q}\right). \quad (15)$$

We immediately see that Eq. (14) yields the exact entropy production in the limit $N_{\text{sites}} \to \infty$. This behavior can be understood, qualitatively, as follows: as the total inter-milestone spacing increases, the relative difference between splitting probabilities such as, e.g., $\phi_{j,+-}$ and $\phi_{j,++}$ becomes negligible because the relative milestone "size" (in the microscopic view) is negligible compared to the milestone territory, which suppresses correlations between entry- and exit-directions to and from the milestone, respectively. In other words, the milestone trajectory approaches a 1st order semi-Markov process. But in the latter case, we expect milestoning to become exact [44].

For the "bare" lumped trajectory we simply set $N_{j,C} = 0$ in the first line of Eq. (14), which gives

$$\langle \dot{S}_1^{\text{aff}}[\hat{x}_{\text{lump}}] \rangle = \frac{1}{N_{\text{sites}} - 1} \langle \dot{S}[x] \rangle. \quad (16)$$

Hence, in the limit $N_{\text{sites}} \to \infty$ the 1st order semi-Markov entropy production estimate in the lumped dynamics vanishes, as observed in Fig. 3d-f.
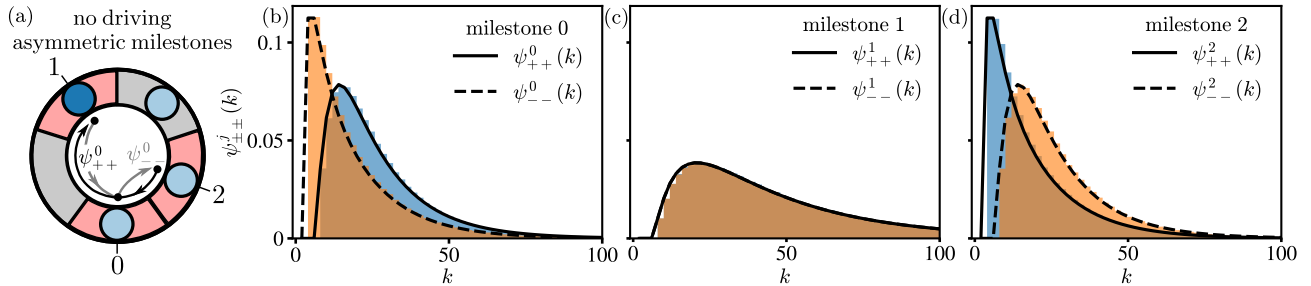
FIG. 5. **Asymmetrically placed milestones result in asymmetric waiting-time distributions irrespective of the driving.** (a) Symmetric single file diffusion, that is, with no driving (i.e., $q = 1/2$), for $N_{\text{sites}} = 5$, and $N_{\text{vac}} = 1$. The three milestones correspond to the positions of the tracer particle (dark blue) indicated in red. (b-d) Waiting-time distributions $\psi^j_{\pm\pm}(k)$ in each of the milestones obtained by simulations (blue + orange) and by Eq. (20) (full + dashed black lines).

SPURIOUS WAITING-TIME CONTRIBUTION AND KINETIC HYSTERESIS

Notably, using Eq. (4) on the uniformly driven single-file system with one vacancy, we recover the exact entropy production, i.e.,

$$\langle \dot{S}_2^{\text{aff}}[\hat{x}_{\text{mil}}] \rangle = \langle \dot{S}_2^{\text{aff}}[\hat{x}_{\text{lump}}] \rangle = \langle \dot{S}[x] \rangle, \quad (17)$$

which we also observe in Fig. 3j-o at $N_{\text{vac}} = 1$.

Importantly, in Eq. (4) we have systematically discarded the waiting-time contribution $\langle \dot{S}_2^{\text{wt}}[\hat{x}_i] \rangle$ that follows from naively applying Eq. (1) to non-Markovian trajectories [41]. A direct computation shows [41]

$$\langle \dot{S}_2^{\text{wt}}[\hat{x}_{\text{mil}}] \rangle = \frac{1}{\langle \tau \rangle} \sum_j \sum_\pm p_{j,\pm\pm} D[\psi^j_{\pm\pm} || \psi^j_{\mp\mp}] \geq 0, \quad (18)$$

where $p_{j,\pm\pm} = \pi_j p_{j,\pm} \phi_{j,\pm\pm}$, and the Kullback-Leibler divergence is given by

$$D[\psi^j_{\pm\pm} || \psi^j_{\mp\mp}] \equiv \sum_{k \geq 1} \psi^j_{\pm\pm}(k) \ln[\psi^j_{\pm\pm}(k)/\psi^j_{\mp\mp}(k)], \quad (19)$$

which is taken between the conditional waiting-time distributions for consecutive forward $\psi^j_{++}(k)$ and backward $\psi^j_{--}(k)$ transitions between milestones. Note that as soon as the conditional forward and backward waiting time distributions are distinct ("asymmetric"), i.e. $\psi^j_{++}(k) \neq \psi^j_{--}(k)$ for some k, Eq. (S1) implies dissipation, irrespective of whether the microscopic dynamics is truly dissipative or not. The conditional waiting-time distributions read [80]

$$\psi^j_{++}(k) = \mathcal{F}_{\Delta_j}(q, \Delta_{j,+}, k)/\phi_{j,++},$$
$$\psi^j_{--}(k) = \mathcal{F}_{\Delta_j}(1 - q, \Delta_{j-1,+}, k)/\phi_{j,--},$$

where we introduced the auxiliary function

$$\mathcal{F}_\Delta(q, z, k) \equiv \frac{2^k}{\Delta}(1 - q)^{\frac{k+z}{2}} q^{\frac{k-z}{2}}$$
$$\times \sum_{l=1}^{\Delta-1} \cos^{k-1}\left(\frac{l\pi}{\Delta}\right) \sin\left(\frac{l\pi}{\Delta}\right) \sin\left(\frac{l\pi z}{\Delta}\right). \quad (20)$$

In Fig. 5 we show that as soon as the distance to the left/right neighboring milestone is not symmetric, we obtain $D[\psi^j_{\pm\pm} || \psi^j_{\mp\mp}] > 0$ and thus it follows from Eq. (17) that $\langle \dot{S}_2^{\text{aff}}[\hat{x}_i] \rangle + \langle \dot{S}_2^{\text{wt}}[\hat{x}_i] \rangle > \langle \dot{S}[x] \rangle$. Moreover, even under perfect (microscopic) detailed balance (i.e., $q=1/2$) we find that the waiting-time distributions are asymmetric (see Fig. 5), and therefore $D[\psi^j_{\pm\pm} || \psi^j_{\mp\mp}] > 0$ and thus $\langle \dot{S}_2^{\text{wt}}[\hat{x}_{\text{mil}}] \rangle > \langle \dot{S}[x] \rangle = 0$. The above 2nd order semi-Markov example and the family of 1st order semi-Markov counterexamples in [15–17] disprove that waiting-times *in general* contribute to dissipation in Eq. (1). The waiting-time contribution in Eq. (S1) in our example quantifies the difference between the waiting-time distributions between forward versus backward transitions, but it does *not* contribute to dissipation.

Note that the post-lumped milestoned process displays kinetic hysteresis (i.e., coarse-graining and time reversal do not commute; see SM) [16], whereas the original lumped dynamics does *not*. For the latter, the waiting-time distributions are symmetric irrespective of the lump sizes and presence or absence of driving, resulting in a vanishing waiting-time contribution $\langle \dot{S}_2^{\text{wt}}[\hat{x}_{\text{lump}}] \rangle = 0$. Therefore, in the presence of kinetic hysteresis in coarse-grained dynamics, the waiting-time contribution in Eq. (S1) does *not* contribute to dissipation, and in its absence it typically (i.e. in our examples) seems to vanish (see, however, non-vanishing contributions in [41]). Therefore, since it is *not* possible in practice to test for the presence of kinetic hysteresis without the knowledge of the full dynamics, asymmetric waiting-time distributions generally *cannot* be used to infer dissipation via Eq. (S1), i.e., there is no implication between the two: $\langle \dot{S}[x] \rangle > 0 \implies \langle \dot{S}^{\text{wt}}[\hat{x}] \rangle > 0$ and in turn $\langle \dot{S}^{\text{wt}}[\hat{x}] \rangle > 0 \implies \langle \dot{S}[x] \rangle > 0$. In fact, using the naive Markovian time-reversal operation $\{\theta \hat{x}_i(\tau)\}_{0 \leq \tau \leq t} \overset{!}{=} \{\hat{x}_i(t - \tau)\}_{0 \leq \tau \leq t}$ in Eq. (1), at least for 1st and 2nd order semi-Markov processes in the presence of kinetic hysteresis, is inconsistent and does *not* describe dissipation correctly. Notably, the complete thermodynamically consistent definition of dissipation for 1st order semi-Markov processes has been established in [16], while for 2nd order semi-Markov pro-

cesses the affinity contribution $\langle \dot{S}_2^{\text{aff}}[\hat{x}] \rangle$ seems to provide a correct lower bound, $\langle \dot{S}[x] \rangle \geq \langle \dot{S}_2^{\text{aff}}[\hat{x}] \rangle$.

DISCUSSION

Correct notion of time reversal.— Contrasting the setting where all hidden degrees of freedom relax instantaneously fast, that is solved essentially completely within the notion of "local detailed balance" [18], inferring dissipation from general coarse observations remains both conceptually and technically challenging and is still understood very poorly. Sufficiently far from equilibrium, challenges appear even in the presence of a time-scale separation between the hidden and observed degrees of freedom [44]. In the absence of such time-scale separation, and for an arbitrary extent of memory, the problem remains unsolved. This is because a correct general mathematical definition of dissipation in the presence of memory is not known. In particular, the definition in Eq. (1) is incomplete, because the correct general form of the time-reversal operation θ remains elusive. Memory reflects (anti-)persistence in dynamics, and it is therefore not surprising that it manifests some abstract analogy to momenta.

Whereas practical methods are available to infer the presence [81, 82] and range [83–85] of memory in coarse observations, the precise flavor of non-Markovianity is typically not known. In particular, if only coarse-grained trajectories are accessible, such as in experimental studies, it is inherently *impossible* to check for the presence of kinetic hysteresis. Therefore, referring to the absence of kinetic hysteresis as a "mild assumption" [86] seems somewhat inappropriate. Either way, since $\langle \dot{S}^{\text{wt}}[\hat{x}] \rangle$ can be positive even under detailed balance, and one cannot check for kinetic hysteresis, a non-vanishing $\langle \dot{S}^{\text{wt}}[\hat{x}] \rangle$ generally cannot be used to infer dissipation.

Even if the order of memory is known, the correct notion of physical time reversal generally remains elusive. For semi-Markov processes of 1$^{\text{st}}$ order it has been proven that the transition-path periods (i.e., the duration of successful transitions between coarse states) are "odd" under time reversal (i.e., transition paths between any pair of states must be reverted in the time-reversed trajectory like momenta in inertial systems), and the thermodynamically consistent time-reversal operation was established [16]. Importantly, by explicit counterexamples it was proven that waiting-time effects in 1$^{\text{st}}$ and 2$^{\text{nd}}$ order semi-Markov processes generally do *not* measure dissipation. Note that reverting all transition paths in the time-reversed trajectories ensures $\langle \dot{S}^{\text{wt}}[\hat{x}] \rangle = 0$, and thus has the same effects as simply ignoring $\langle \dot{S}^{\text{wt}}[\hat{x}] \rangle$. Moreover, we found that for the 2$^{\text{nd}}$ order semi-Markov process with no hidden dissipative cycles [87] in Fig. 3 (see also [17, 44]), the two-step affinity exactly recovers the microscopic dissipation, which requires all waiting time contributions to be systematically discarded. To what extent and under which conditions this, i.e., $\langle \dot{S}^{\text{aff}}[\hat{x}_i] \rangle = \langle \dot{S}[x] \rangle$

in the absence of hidden cycles, is true for general k^{th} order semi-Markov processes ($k > 2$) still needs to be established. Whether a general form of time reversal θ exists that would always yield a consistent waiting-time contribution to dissipation remains unknown. One can construct 2$^{\text{nd}}$ (but not 1$^{\text{st}}$) order semi-Markov processes without kinetic hysteresis that have asymmetric waiting time distributions whose contribution does not violate the inequality (2) [41]. However, our results show that for 1$^{\text{st}}$ and 2$^{\text{nd}}$ order semi-Markov processes waiting-time effects as encoded in $\langle \dot{S}^{\text{wt}}[\hat{x}] \rangle$ are either nominally zero or else must be discarded, since one cannot know (nor can one test) for the presence of kinetic hysteresis without the knowledge of microscopic dynamics. We believe this to be a result of an incorrect or incomplete definition of time-reversal θ when applying Eq. (1) to 1$^{\text{st}}$ and 2$^{\text{nd}}$ order semi-Markov processes. We expect this to also be true for processes with longer memory, where, however, evaluating the path probabilities becomes challenging.

Practical aspects of milestoning.— From a practical perspective, one therefore does not generally know how to correctly apply Eq. (1) to infer dissipation from observed non-Markovian trajectories. A convenient, practical, and consistent approach we push forward here is to first milestone trajectories and thereafter assume 1$^{\text{st}}$ or 2$^{\text{nd}}$ order semi-Markov correlations in the evaluation of Eq. (1) excluding any waiting-time contributions. Even if this assumption is not satisfied exactly (i.e., the memory is actually longer-ranged), a *meaningful* milestoning will systematically render the observations "closer" to the underlying microscopic dynamics and thus improve thermodynamic inference. Moreover, a sparser placement of milestones increases the accuracy of inference and is numerically more efficient.

One is therefore tempted to think that milestones should generally be placed as sparsely as possible for optimal thermodynamic inference. There is, however, a practical limitation. Consider the example of observing a tracer particle in a single-file. If we increase the spacing between milestones, the estimate for $\langle \dot{S}[\hat{x}_{\text{mil}}] \rangle$ per milestone transition indeed gradually improves (i.e., increases). At large distances between milestones, however, the sequence of visited milestones will appear nearly deterministic, whereby transitions against the driving (i.e., "time-reversed trajectory segments") will become increasingly unlikely. Thus, the evaluation of Eq. (1) using trajectory-derived path probabilities will require better and better sampling (see the SM for a quantitative statement). Analytical estimates of transition probabilities (such as presented here) are of course not affected. In general, the placement of milestones should be optimized as a trade-off between accuracy and statistical feasibility.

Finally, we stress that the proposed post-lumped milestoning based thermodynamic inference requires at least one dissipative cycle to be observable. If some dissipative cycles are hidden by the coarse-graining, milestoning based estimation will yield a *true* lower bound on dissipation. However, if truly *all* dissipative cycles become

hidden, the method will fail, and one should resort to alternative "transition-based" approaches developed recently [19–22] to infer some lower bound on dissipation.

Author contributions.—A.G. and D.E.M. conceived the research and drafted the manuscript. K.B. wrote the computer program and performed the analytical and numerical calculations. K.S. and E.V. contributed to theory development and provided critical feedback on the manuscript. All authors contributed to the interpretation of the results, and the writing of the manuscript.

Competing interests.— The authors declare that they have no competing interests.

Data availability.— The raw data and source codes to reproduce the results shown in this manuscript are publicly available at [58].

[1] R. Yasuda, H. Noji, M. Yoshida, K. Kinosita Jr, and H. Itoh, Nature **410**, 898 (2001).

[2] A. Godec and D. E. Makarov, J. Phys. Chem. Lett. **14**, 49 (2023).

[3] C. Ratzke, B. Hellenkamp, and T. Hugel, Nat. Commun. **5**, 4192 (2014).

[4] Y. Tu, Proc. Natl. Acad. Sci. U.S.A. **105**, 11737 (2008).

[5] F. S. Gnesotto, F. Mura, J. Gladrow, and C. P. Broedersz, Rep. Prog. Phys. **81**, 066601 (2018).

[6] J. Li, J. M. Horowitz, T. R. Gingrich, and N. Fakhri, Nat. Commun. **10**, 1666 (2019).

[7] D. E. Makarov, *Single molecule science: physical principles and models* (CRC Press, 2015).

[8] J. Mehl, B. Lander, C. Bechinger, V. Blickle, and U. Seifert, Phys. Rev. Lett. **108**, 220601 (2012).

[9] C. Dieball and A. Godec, Phys. Rev. Lett. **129**, 140601 (2022).

[10] N. Q. Hoffer and M. T. Woodside, Curr. Opin. Chem. Biol. **53**, 68 (2019).

[11] B. Schuler and W. A. Eaton, Curr. Opin. Struct. Biol. **18**, 16 (2008).

[12] H. S. Chung and W. A. Eaton, Curr. Opin. Struct. Biol. **48**, 30 (2018).

[13] L. Peliti and S. Pigolotti, *Stochastic Thermodynamics: An Introduction* (Princeton University Press, 2021).

[14] U. Seifert, Rep. Prog. Phys. **75**, 126001 (2012).

[15] H. Wang and H. Qian, J. Math. Phys. **48**, 013303 (2007).

[16] D. Hartich and A. Godec, Phys. Rev. X **11**, 041047 (2021).

[17] D. Hartich and A. Godec, "Comment on "inferring broken detailed balance in the absence of observable currents"," (2022), arXiv:2112.08978 [cond-mat.stat-mech].

[18] M. Esposito, Phys. Rev. E **85**, 041125 (2012).

[19] J. van der Meer, B. Ertel, and U. Seifert, Phys. Rev. X **12**, 031025 (2022).

[20] P. E. Harunari, A. Dutta, M. Polettini, and E. Roldán, Phys. Rev. X **12**, 041026 (2022).

[21] J. van der Meer, J. Degünther, and U. Seifert, Phys. Rev. Lett. **130**, 257101 (2023).

[22] J. Degünther, J. van der Meer, and U. Seifert, "Fluctuating entropy production on the coarse-grained level: Inference and localization of irreversibility," (2023), arXiv:2309.07665 [cond-mat.stat-mech].

[23] In case of a perfect time-scale separation between the observed and hidden degrees of freedom, the total entropy production is not necessarily underestimated by a coarse-grained representation.

[24] Q. Yu, D. Zhang, and Y. Tu, Phys. Rev. Lett. **126**, 080601 (2021).

[25] A. Puglisi, S. Pigolotti, L. Rondoni, and A. Vulpiani, J. Stat. Mech. **2010**, P05015 (2010).

[26] G. Teza and A. L. Stella, Phys. Rev. Lett. **125**, 110601 (2020).

[27] P. Talkner and P. Hänggi, Rev. Mod. Phys. **92**, 041002 (2020).

[28] A. C. Barato and U. Seifert, Phys. Rev. Lett. **114**, 158101 (2015).

[29] J. M. Horowitz and T. R. Gingrich, Nat. Phys. **16**, 15 (2019).

[30] T. R. Gingrich, G. M. Rotskoff, and J. M. Horowitz, J. Phys. A: Math. Theor. **50**, 184004 (2017).

[31] T. V. Vu, V. T. Vo, and Y. Hasegawa, Physical Review E **101**, 042138 (2020).

[32] S. K. Manikandan, D. Gupta, and S. Krishnamurthy, Phys. Rev. Lett. **124**, 120603 (2020).

[33] S. Otsubo, S. Ito, A. Dechant, and T. Sagawa, Phys. Rev. E **101**, 062106 (2020).

[34] J. Li, J. M. Horowitz, T. R. Gingrich, and N. Fakhri, Nat. Commun. **10**, 1666 (2019).

[35] T. Koyuk and U. Seifert, J. Phys. A: Math. Theor. **54**, 414005 (2021).

[36] C. Dieball and A. Godec, Phys. Rev. Research **4**, 033243 (2022).

[37] A. Dechant and S.-i. Sasa, Phys. Rev. Research **3**, 042012 (2021).

[38] A. Dechant and S.-i. Sasa, Phys. Rev. X **11**, 041061 (2021).

[39] C. Dieball and A. Godec, Phys. Rev. Lett. **130**, 087101 (2023).

[40] U. Seifert, Physica A **504**, 176 (2018).

[41] I. A. Martínez, G. Bisker, J. M. Horowitz, and J. M. Parrondo, Nat. Commun. **10**, 3542 (2019).

[42] J. Ehrich, J. Stat. Mech. Theory Exp. **2021**, 083214 (2021).

[43] D. J. Skinner and J. Dunkel, Phys. Rev. Lett. **127**, 198101 (2021).

[44] D. Hartich and A. Godec, Phys. Rev. Res. **5**, L032017 (2023).

[45] J. M. Bello-Rivas and R. Elber, J. Chem. Phys. **142**, 094102 (2015).

[46] R. Elber, J. Chem. Phys. **144**, 060901 (2016).

[47] R. Elber, D. E. Makarov, and H. Orland, *Molecular ki-*

netics in condensed phases: theory, simulation, and analysis (John Wiley & Sons, 2020).

[48] C. Schütte, F. Noé, J. Lu, M. Sarich, and E. Vanden-Eijnden, J. Chem. Phys. **134**, 204105 (2011).

[49] B. Ertel, J. van der Meer, and U. Seifert, Phys. Rev. E **105**, 044113 (2022).

[50] G. Teza and A. L. Stella, Phys. Rev. Lett. **125**, 110601 (2020).

[51] E. Nitzan, A. Ghosal, and G. Bisker, "Universal bounds on entropy production inferred from observed statistics," (2022), arXiv:2212.01783 [cond-mat.stat-mech].

[52] M. Uhl, P. Pietzonka, and U. Seifert, J. Stat. Mech. Theory Exp. **2018**, 023203 (2018).

[53] M. Polettini, A. Wachtel, and M. Esposito, J. Chem. Phys. **143**, 184103 (2015), https://pubs.aip.org/aip/jcp/article-pdf/doi/10.1063/1.4935064/15504178/184103_1_online.pdf.

[54] K. H. Choo, J. C. Tong, and L. Zhang, Genomics Proteomics Bioinformatics **2**, 84 (2004).

[55] M. Delorenzi and T. Speed, Bioinformatics **18**, 617 (2002).

[56] E. Roldán and J. M. R. Parrondo, Phys. Rev. Lett. **105**, 150607 (2010).

[57] E. Roldán and J. M. R. Parrondo, Phys. Rev. E **85**, 031129 (2012).

[58] K. Blom, K. Song, E. Vouga, A. Godec, and D. E. Makarov, https://gitlab.gwdg.de/kblom/milestoning-estimators-for-entropy-production (2023).

[59] T. E. Harris, J. Appl. Prob. **2**, 323 (1965).

[60] J. L. Lebowitz and J. K. Percus, Phys. Rev. **155**, 122 (1967).

[61] E. Barkai and R. Silbey, Phys. Rev. Lett. **102**, 050602 (2009).

[62] N. Leibovich and E. Barkai, Phys. Rev. E **88**, 032107 (2013).

[63] A. Lapolla and A. Godec, New J. Phys. **20**, 113021 (2018).

[64] A. Lapolla and A. Godec, J. Chem. Phys. **153**, 194104 (2020).

[65] D. Hartich and A. Godec, Phys. Rev. Lett. **127**, 080601 (2021).

[66] O. Bénichou, P. Illien, G. Oshanin, A. Sarracino, and R. Voituriez, J. Physics: Cond. Matt. **30**, 443001 (2018).

[67] P. Illien, O. Bénichou, C. Mejía-Monasterio, G. Oshanin, and R. Voituriez, Phys. Rev. Lett. **111**, 038102 (2013).

[68] T. Bertrand, P. Illien, O. Bénichou, and R. Voituriez, New J. Phys. **20**, 113045 (2018).

[69] J. Shin, A. M. Berezhkovskii, and A. B. Kolomeisky, J. Phys. Chem. Lett. **11**, 4530 (2020).

[70] I. M. Sokolov, Soft Matter **8**, 9043 (2012).

[71] G. Hummer, J. C. Rasaiah, and J. P. Noworyta, Nature **414**, 188 (2001).

[72] S. F. Burlatsky, G. Oshanin, M. Moreau, and W. P. Reinhardt, Phys. Rev. E **54**, 3165 (1996).

[73] I. Lobaskin, M. R. Evans, and K. Mallick, J. Phys. A Math. Theor. **55**, 205002 (2022).

[74] A. Miron and D. Mukamel, J. Phys. A Math. Theor. **54**, 025001 (2020).

[75] A. Miron, D. Mukamel, and H. A. Posch, J. Phys. A Math. Theor. **2020**, 063216 (2020).

[76] A. Kundu and J. Cividini, EPL **115**, 54003 (2016).

[77] T. Banerjee, R. L. Jack, and M. E. Cates, J. Stat. Mech. Theory Exp. **2022**, 013209 (2022).

[78] K. Proesmans and C. V. den Broeck, EPL **119**, 20001 (2017).

[79] J. Vrbik, Math. J. **14**, 1 (2012).

[80] W. Feller, *An introduction to probability theory and its applications, Volume 2*, Vol. 81 (John Wiley & Sons, 1991).

[81] A. M. Berezhkovskii and D. E. Makarov, J. Phys. Chem. Lett. **9**, 2190–2195 (2018).

[82] K. Engbring, D. Boriskovsky, Y. Roichman, and B. Lindner, Phys. Rev. X **13**, 021034 (2023).

[83] A. Lapolla and A. Godec, Phys. Rev. Res. **3**, L022018 (2021).

[84] K. Song, D. E. Makarov, and E. Vouga, Phys. Rev. Res. **5**, L012026 (2023).

[85] K. Song, R. Park, A. Das, D. E. Makarov, and E. Vouga, J. Chem. Phys. **159**, 064104 (2023).

[86] F. A. Cisneros, N. Fakhri, and J. M. Horowitz, J. Stat. Mech. **2023**, 073201 (2023).

[87] A dissipative cycle in a Markov process is a cycle for which the Kolmogorov cycle criterion is violated. The cycle is said to be hidden if the states of said cycle are coarse-grained into the same lump.

Supplemental Material for:
Milestoning estimators of dissipation in systems observed at a coarse resolution: When ignorance is truly bliss

In this Supplementary Material (SM) we present details and further extensions of the results shown in the main manuscript.

A. Toy model for a higher-order semi-Markov process

In Fig. S1a we extend the toy model for a 2nd order semi-Markov process introduced in the main manuscript. The extension includes an additional exit and entrance connection between the lumped states with different transition rates $\{w^{\dagger}_{\text{lump},+}, w^{\dagger}_{\text{lump},-}\}$. In Fig. S1b-c we observe that milestoning the lumped trajectory significantly improves the entropy production estimate within the 1st order semi-Markov approximation. On the 2nd order semi-Markov level, milestoning does not improve nor deteriorate the entropy-production estimate.
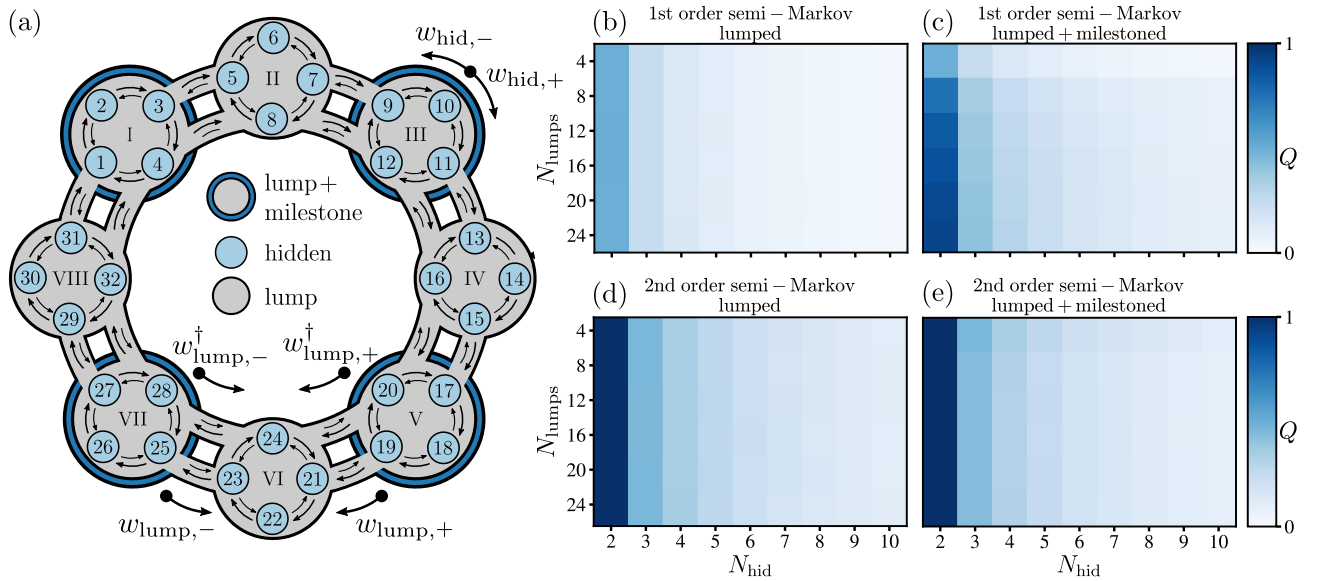

FIG. S1. **Entropy production inference for a semi-Markov process beyond 2nd order** (a) Schematic of the toy model with 32 microstates lumped into domains I-VIII (gray) each containing 4 microstates. Milestoning involves further post-processing of the lumped process: some lumped states (here, the domains I, III, V, and VII) are declared to be milestones (blue). Once the trajectory enters a milestone, the coarse-grained state of the milestone trajectory remains in said milestone until it enters a different milestone. (b-e) Estimating the entropy production from a coarse-grained trajectory governed by the discrete-state ring-like Markov chain shown in (a), with N_{lumps} the number of lumped states, N_{hid} the number of hidden microstates per lumped state, transition rates $\{w_{\text{lump},+}, w_{\text{lump},-}\} = \{w_{\text{hid},+}, w_{\text{hid},-}\} = \{0.52, 0.48\}$, $\{w^{\dagger}_{\text{lump},+}, w^{\dagger}_{\text{lump},-}\} = \{0.51, 0.49\}$, and 10^8 discrete steps. (b, d) Quality factor Q (see Eq. (5) in manuscript) for the entropy production estimated with the lumped trajectory assuming 1st order semi-Markov (see Eq. (3) in manuscript) (b) and 2nd order semi-Markov (see Eq. (4) in manuscript) (d). (c, e) Quality factor for the entropy production estimated with the post-lumped milestoned trajectory with 4 equidistant milestones, assuming 1st order semi-Markov (c) and 2nd order semi-Markov (e).

B. Waiting-time contribution in the ring process

In Fig. S2 we show the waiting-time distributions for the toy models shown in Fig. 1a in the main manuscript and Fig. S1a in the SM. For both models, we take 3 milestones which are placed asymmetrically, i.e. the milestones are *not* placed equidistantly as shown in Fig. S2a,e. Furthermore, we take fully symmetric transition rates $w_{\text{hid},+} = w_{\text{lump},+} = w^{\dagger}_{\text{lump},+} = w_{\text{hid},-} = w_{\text{lump},-} = w^{\dagger}_{\text{lump},-} = 1/2$, which renders both, the exact microscopic result as well as the affinity entropy estimate zero, i.e. $\langle \dot{S}[x] \rangle = \langle \dot{S}^{\text{aff}}_2[\hat{x}_{\text{lump}}] \rangle = \langle \dot{S}^{\text{aff}}_2[\hat{x}_{\text{mil}}] \rangle = 0$. In Fig. S2b-d and f-h we observe that the waiting-time distributions $\psi_{++}(k)$ and $\psi_{--}(k)$ for milestones VII and V are unequal (compare orange and blue

histograms). This renders the waiting-time contribution to the entropy production nonzero, i.e., (note that the index j sums over the 3 milestones)

$$\langle \dot{S}_2^{\mathrm{wt}}[\hat{x}_{\mathrm{mil}}]\rangle = \frac{1}{\langle\tau\rangle}\sum_j\sum_{\pm} p_{j,\pm\pm} D[\psi_{\pm\pm}^j || \psi_{\mp\mp}^j] \geq 0. \tag{S1}$$

Therefore, by incorporating Eq. (S1) in the total estimate for the entropy production, one would mistakenly conclude that this system (which strictly obeys detailed balance) has dissipative fluxes, which is clearly not the case.

C.   Inference via the Thermodynamic Uncertainty Relation

Fig. 3p-u in the main manuscript depicts the inference of the entropy production rate in a single-file system using the discrete-time thermodynamic uncertainty relation (TUR). The discrete-time TUR reads [1]

$$\langle \dot{S}_{\mathrm{TUR}}\rangle = \ln\left(2\langle J_i\rangle^2/\mathrm{var}(J_i) + 1\right), \tag{S2}$$

where $\langle J_i\rangle$ and $\mathrm{var}(J_i)$ are the average and variance, respectively, of the tracer-particle current in the lumped and post-lumped milestoned trajectories. To determine the current in the lumped and post-lumped milestones trajectories $\hat{x}_i(t)$, we simply take the difference between two consecutive jumps, i.e.,

$$J_i(t) = \hat{x}_i(t) - \hat{x}_i(t-1), \tag{S3}$$

where the difference is taken modulo the number of sites ($i = \mathrm{lump}$) or milestones ($i = \mathrm{mil}$). The mean and variance of the current are then determined via

$$\langle J_i\rangle = \frac{1}{T}\sum_{t=1}^{T} J_i(t), \ \mathrm{var}(J_i) = \frac{1}{T}\sum_{t=1}^{T}(J_i - \langle J_i\rangle)^2, \tag{S4}$$

where T is the total number of steps in the trajectory. For the results shown in Fig. 3p-u in the main manuscript we have $T = 10^8$.
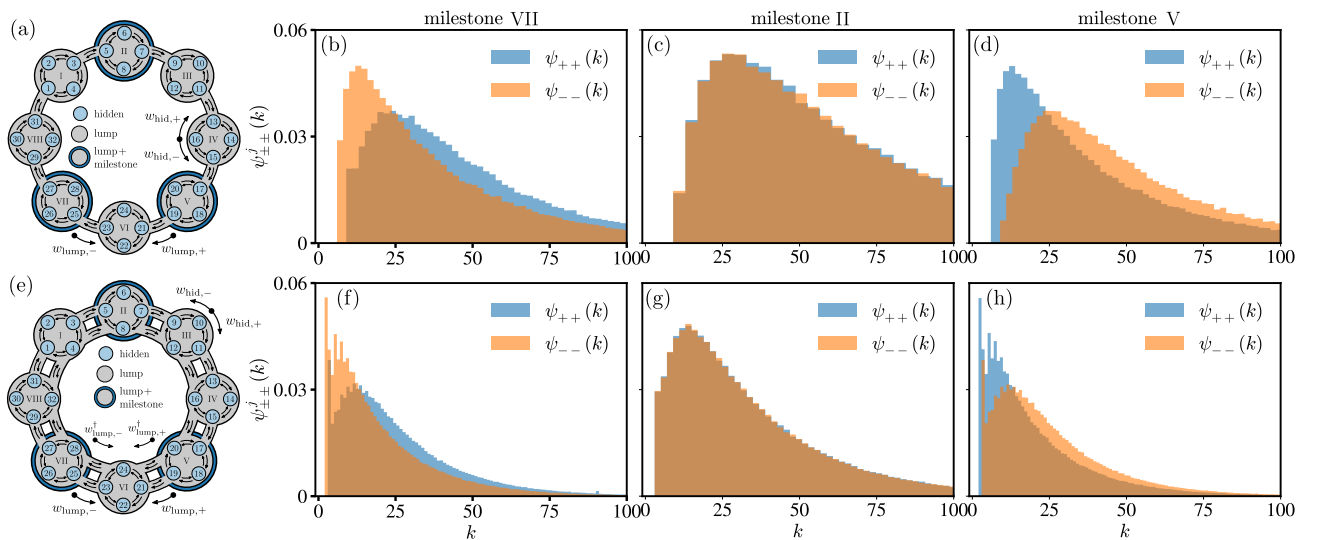

FIG. S2. **Waiting-time distribution for 3 asymmetrically placed milestones in the ring process with detailed-balance.** In all panels, we consider symmetric transition rates (inside the lumps and those connecting the different lumps) $w_{\mathrm{hid},+} = w_{\mathrm{lump},+} = w_{\mathrm{lump},+}^\dagger = w_{\mathrm{hid},-} = w_{\mathrm{lump},-} = w_{\mathrm{lump},-}^\dagger = 1/2$ for the ring process with $N_{\mathrm{lump}} = 8$, $N_{\mathrm{hid}} = 4$, and milestones placed at lumps {II, V, VII}. Waiting-time distributions are obtained from a stochastic trajectory with 10^8 discrete steps. (a-d) Waiting-time distributions for the toy model introduced in Fig. 1a in the main manuscript. (e-h) Waiting-time distributions for the toy model introduced in Fig. S1a in the SM.
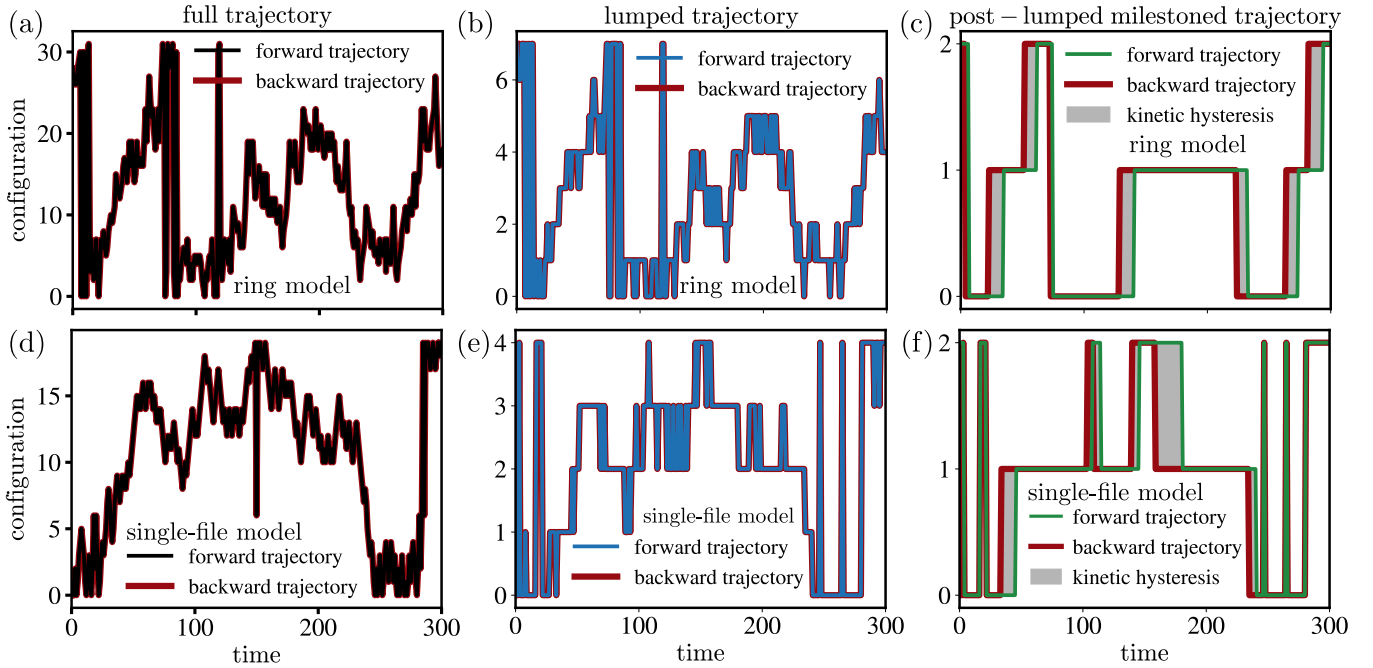
FIG. S3. **Stochastic trajectories and kinetic hysteresis in the ring model and single-file system.** For the ring model, we consider $N_{\mathrm{lump}} = 8$ lumped macrostates, and $N_{\mathrm{hid}} = 4$ hidden microstates per lump. For the single-file system, we consider $N_{\mathrm{sites}} = 5$ sites, and $N_{\mathrm{vac}} = 1$ vacancies. Backward trajectories are indicated with the solid red line. (a, d) Microscopic stochastic trajectories. (b, e) Lumped stochastic trajectories. (c, f) Milestoned stochastic trajectories. The gray shaded area denotes the kinetic hysteresis where forward and backward trajectories differ.

D. Milestoning and kinetic hysteresis

A fundamental difference between lumping and milestoning is that for the latter, time reversal and coarse-graining do not commute, which was coined "kinetic hysteresis" [2]. To see this, let us consider a stochastic trajectory for the ring model (see Fig. 1a in the main manuscript) and single-file system (see Fig. 3 in the main manuscript), as shown in Fig. S3. In Fig. S3a,d we display the microscopic stochastic trajectories, for which the forward (black line) and backward (red line) trajectories are identical under time inversion. For the lumped trajectories, shown in Fig. S3b,e we also find that the backward trajectories traverse along identical paths under time inversion. However, it turns out that the milestoned trajectories depicted in Fig. S3c,f display the following phenomenon [2]: If we coarse grain the same trajectory backward in time, we discover a kinetic hysteresis. That is, the time-reversed coarse trajectory (red line in Fig. S3c,f), where time is running from right to left, differs from the forward one (green line in Fig. S3c,f). Hence, using the naive Markovian time-reversal operation θ

$$\{\theta \hat{x}_i(\tau)\}_{0 \leq \tau \leq t} \overset{!}{=} \{\hat{x}_i(t - \tau)\}_{0 \leq \tau \leq t} \quad \perp \tag{S5}$$

in the presence of kinetic hysteresis is inconsistent and does *not* describe dissipation upon inserting into Eq. (1) in the manuscript.

E. "Statistical burden" of improving thermodynamic inference via milestoning

In the main manuscript, we pointed out that there is a practical limitation to milestoning a lumped trajectory, which is due to the fact that for increasing milestone distances the estimation of the entropy production requires more sampling. In Fig. S4 we show this explicitly for a uniformly biased single-file system with $N_{\mathrm{vac}} = 1$ and $N_{\mathrm{sites}} = 9$. Upon comparing the entropy production estimates for the lumped trajectory (Fig. S4a,b) with the milestoned trajectory (Fig. S4c,d), we find that convergence of the latter requires much longer trajectories. This is because larger inter-milestone distances render transitions against the driving increasingly unlikely. We further observe in Fig. S4b,d that for insufficient sampling, the estimated entropy production can exceed the true entropy production (indicated with the black dashed line) for both lumping and milestoning. Hence, it is always important

that sufficiently long (and/or many) trajectories are provided to estimate the entropy production.
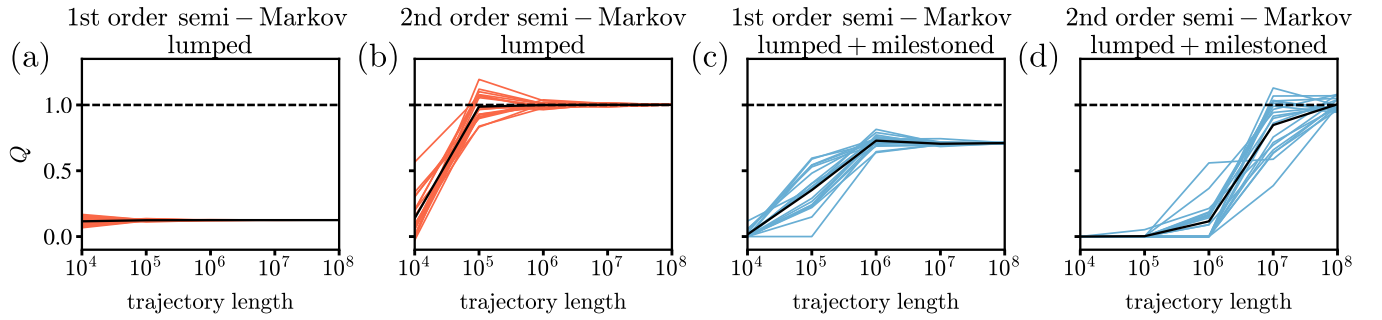

FIG. S4. **Improved thermodynamic inference via milestoning demands better trajectory statistics.** In all panels we consider a uniformly biased single-file system with $N_{\text{vac}} = 1$, $N_{\text{sites}} = 9$, $w_+ = 0.46$, and 3 maximally separated milestones. Colored lines are obtained from 20 individual trajectories, and the black solid line shows the average. (a-b) Quality factor for the entropy production estimate in the lumped trajectory, based on the 1st (a) and 2nd (b) order semi-Markov approximation. (c-d) Quality factor for the entropy production estimate in the post-lumped milestoned trajectory, based on the 1st (c) and 2nd (d) order semi-Markov approximation.

[1] K. Proesmans and C. V. den Broeck, EPL **119**, 20001 (2017).
[2] D. Hartich and A. Godec, Phys. Rev. X **11**, 041047 (2021).